euspen's 22nd International Conference & Exhibition, Geneva, CH, May/June 2022
www.euspen.eu

Improving form accuracy in ultra-precision machining of calcium fluoride by integrating vibration-assisted cutting and coating technology

Yan Jin Lee

Department of Mechanical Engineering, National University of Singapore, 9 Engineering Drive 1, Singapore 117575, Singapore

**lionel.lyj@u.nus.edu*

Abstract
Modern machine tools are highly capable of ultra-precise tool positioning to manufacture desired structures conforming to intended design requirements. However, elastic recovery of machined surfaces creates a roadblock toward the goal of achieving high form accuracy as shown by a 63.0% post-scratching elastic recovery on single-crystal calcium fluoride. While ultrasonic elliptical vibration-assisted machining (UEVAM) is a proven success at promoting ductile-mode cutting and improving form accuracy, an 18.6% elastic recovery of the machined surface was still prevalent. The integration of UEVAM with a relatively new method to improve the machinability of brittle materials by pre-coating the sample surface further reduces the deviation of the machined surface from the designed profile to 5.0%. In addition to affecting form accuracy, the elastic recovered material also led to the increase in thrust forces by 21.1% without the influence of the coating. It was suggested that the coating intensified the concentration of stress in the primary deformation zone to activate secondary slip systems that accounted for a large proportion of the cutting energy in the region, which consequently reduced the stress acting on the machined surface leading to lower deformation of the subsurface and its recovery. This work presents an optimistic combination of advanced techniques to augment the form accuracy in ultra-precision machining.

Keywords: ultra-precision machining, calcium fluoride, epoxy coating, vibration-assisted machining, form accuracy

1. Introduction

Advances in ultra-precision machining technology can fulfil the stringent requirements of precision engineering products, which include surface finishing and form accuracy. However, the elastic recovery of the machined surface remains an issue resulting in the deviation of the final surface from the intended design. Thus, this work aims to evaluate the integration of two advanced methods to augment micro-cutting and address this issue.

Ultrasonic elliptical vibration-assisted machining (UEVAM) is well established to bring micro-cutting with multiple benefits [1]. One critical outcome is the improved surface finish on brittle materials [2] owing to the incremental material removal in each elliptical motion of the cutting tool. On the cutting of brittle materials, a recent finding in coating the sample surface prior to cutting was reported to also enhance ductile-mode cutting due to additional stresses induced into the workpiece by the deformed coating layer [3]. It is consequently of interest to capitalize on the effectiveness of UEVAM to promote ductile-mode cutting and the change in stress during cutting of the coated workpiece to address the issue of elastic recovery on the machined surface. Therefore, this work will perform a series of experiments by first validating the elastic recovery of CaF_2, followed by micro-cutting tests to evaluate the integration of vibration-assisted cutting and the pre-coating of the workpiece.

2. Experiments

2.1. Micro-scratch tests

An MCT^3 micro-scratch tester from Anton Paar was employed to perform linear-load scratching on the (100) plane of a CaF_2 sample. The benefit of using this system is that all measurements were relative to the initial sample surface. A pre-scan of the workpiece determined the initial surface before the scratch test where the penetration depth was measured relative to the initial surface. Subsequently, a post-scan of the groove was applied to determined the elastically recovered surface. The load linearly increased from 0.03–2 N over a 1 mm scratch length while the penetration depth was concurrently measured during the scratch. A Rockwell indenter with a radius of 100 µm was used for the scratch tests at a constant scratch speed of 10 mm/min.

2.2. Micro-cutting tests

Micro-cutting on the CaF_2 sample was performed on a Toshiba ULG-100 ultra-precision machine center. Diamond turning was first performed using a 1.6 mm round-nosed single-crystal diamond cutting tool to prepare a flat sample surface prior to further testing. A feed of 1 µm/rev and a nominal cutting depth of 10 µm was set to trim the surface with oil mist as coolant.

Subsequently, an elaborate sequence of procedures was employed to effectively study the machining accuracy of the integrated methodology. The cutting setup (Figure 1(a)) was equipped with a Kistler 9256C1 dynamometer and Type 5051 amplifiers to measure cutting forces and an ultrasonic elliptical vibration-assisted machining (UEVAM) tool holder.

Plunge-cutting under the conventional cutting condition was performed to determine the critical uncut chip thickness (i.e., the ductile–brittle transition) prior to further testing using the ultrasonic vibration-assisted machining setup. A 0.4 mm round-nosed polycrystalline diamond (PCD) cutting tool (Figure 1(c)) was set to penetrate the CaF_2 sample at a tapered angle to a final depth of 2 µm. Subsequently, the machined groove was evaluated using a laser confocal microscope (Olympus LEXT OLS5000) to determine the effective depth where cracks begin to appear as 0.3 µm as shown in the scanned profile of the plunge-cut (Figure 2). This ductile–brittle transition point was

then used as a reference cutting depth for the selection of parameters in subsequent UEVAM tests.

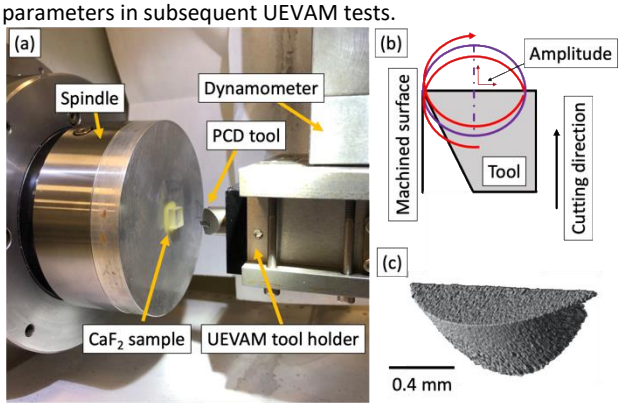

Figure 1. Cutting experiments: (a) Ultrasonic elliptical vibration-assisted cutting setup; (b) illustration of tool-vibration; (c) round-nosed cutting tool edge

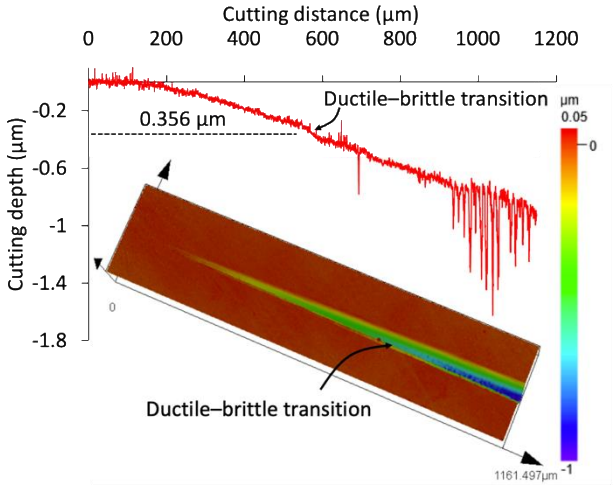

Figure 2. Measured plunge-cut profile and identification of the critical uncut chip thickness

2.3. Vibration-assisted cutting

The two-part type bisphenol-amine epoxy resin was mixed and left to cure on half of the sample (Figure 3(a)) for 30 mins leaving the other half uncoated (Figure 3(b)). Subsequently, the layer of epoxy was diamond turned to produce a coating with a thickness of approximately 4 µm on the CaF_2 surface as measured using the laser confocal microscope (Figure 3(c)). As UEVAM is expected to yield ductile-mode cutting with higher cutting depths (i.e., greater than 0.3 µm), vibration-assisted cutting tests were performed along the same cutting direction of the coated and uncoated regions of the single crystal at a constant depth of 0.5 µm and cutting speed of 50 mm/min. Additionally, tests were performed with varying amplitudes (0, 1, and 2 µm) of the ultrasonic elliptical motion occurring at 38.87 kHz. The elliptical motion of the tool was two-dimensional where the tool vibrated along the axes of the cutting and thrust forces as shown in Figure 1(b). Lastly, the profile of the groove was measured using the laser confocal microscope to be compared with the intended geometry.

3. Results and discussion

3.1. Elastic recovery

The elastic recovery was calculated relative to the reference profile (Ri), penetration depth (Pd), and the residual depth (Rd) as follows:

$$E_r = \frac{Pd - Ri}{Pd} \times 100\% \quad (1)$$

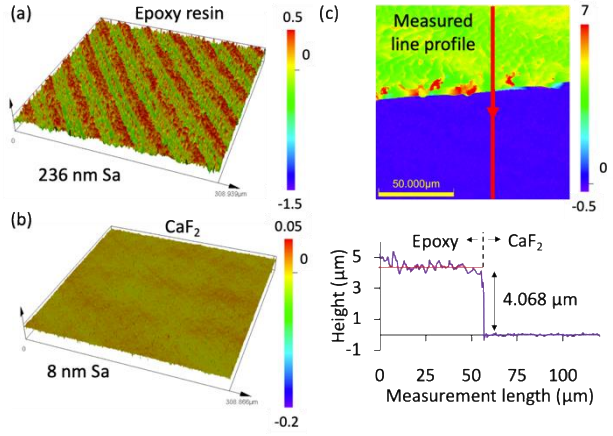

Figure 3. Epoxy coating preparation: (a) illustration of coated regions; (b) measured coating thickness

Figure 4 depicts the top view of scratched grooves (Figure 4(a)) and the measured penetration depths and final surface profile (Figure 4(b)). The deformed surface is observed to elastically recover by a consistent 63%, which demonstrates the potential hindrance of the natural material characteristics to affect the machining accuracy. In the meantime, it is important to recall that the scratch indenter had a 100 µm radius, which would manifest as a significantly large negative rake angled tool when scratching at these depths. Hence, the elastic recovery derived from the scratch tests cannot be directly associated with the recovery from machining.

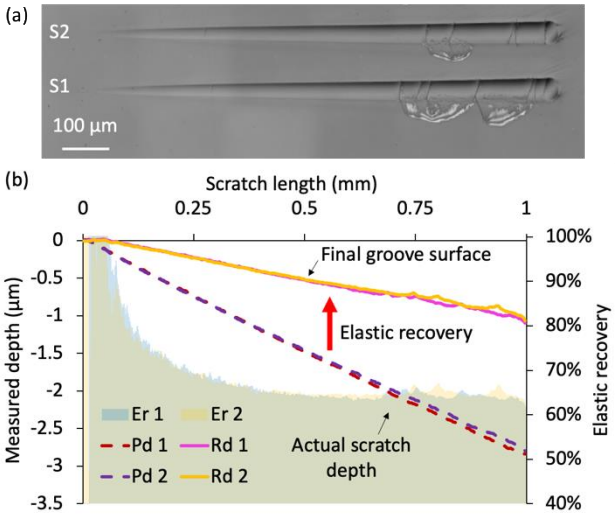

Figure 4. Linear-load scratches, S1 and S2: (a) laser scanned optical top view of the grooves; (b) measured penetration depths (Pd), final surface profile (Rd), and the % recovery of the surface (Er)

3.2. Groove profile

Figure 5(a) depicts the micro-groove produced by integrating UEVAM with the coating where the cross-sectional line profile of the groove is reflected in Figure 5(b). Imperfect machined surfaces of the grooves are visible from the top view images, which appear as an irregular surface with randomly occurring peaks and valleys throughout the curvature of the tool impression. While these micro-features may be often associated with micro-crack formation, the profile is repeatable between grooves (i.e., the same profile appears for different grooves under different cutting conditions). Hence, these irregularities on the surface are attributed to the poor surface quality of the

PCD cutting tool resembling abrasives of a microgrinding tool and should not affect the subject of discussion on the effect of an applied coating on machining form accuracy.

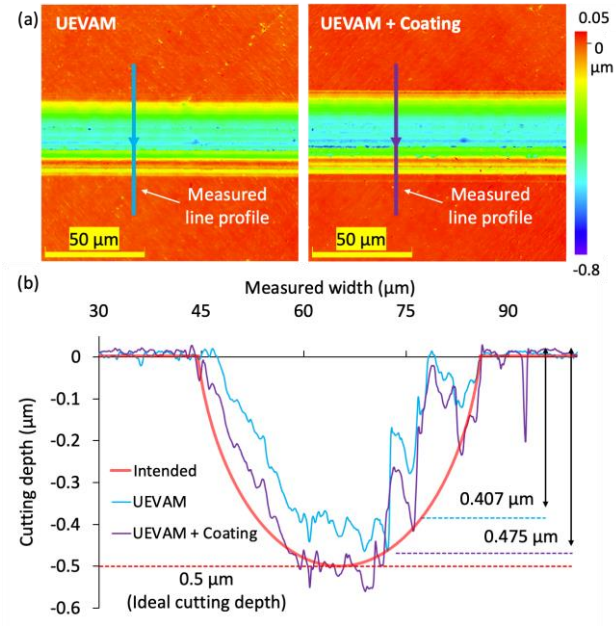

Figure 5. Orthogonal ultrasonic vibration-assisted cutting with and without coating: (a) top view surface height profile of the machined grooves; (b) cross-sectional line measurement of the groove profile

The width of the groove produced by UEVAM and the coating is evidently larger than the groove produced solely by UEVAM (Figure 5(a)). The final depth of the groove produced by the latter measures to an average of 0.407 ± 0.004 µm, which corresponds to an elastic recovery of 18.6%.

On the other hand, the groove produced by vibration-assisted cutting of the coated sample has a machined depth of 0.475 ± 0.001 µm that correspond to a 5.0% deviation of the surface from the intended geometry. This simple test result demonstrates the benefit of coupling the two augmentations for micro-cutting in addressing a critical aspect of ultra-precision machining – form accuracy.

3.3. Machining forces

Figure 6 shows the machining forces, which have been processed by applying a fast Fourier transform (FFT) low-pass filter to remove ultrasonic vibration-induced signals and display data below a frequency of 1.1 kHz. As expected, the cutting forces were recorded to be higher by 64.8% (Figure 6) for the coated sample due to the additional layer of material being removed.

Interestingly, the thrust forces show an opposite trend where the coating resulted in a 21.1% decrease in thrust force, which is unlike the observations in a conventional cutting where the cutting of the coated sample results in the increase of both cutting and thrust forces [3]. While the thrust forces during vibration-assisted cutting are largely associated with friction [4], the solidified coating is unlikely to promote the reduction in coefficient of friction at the tool-chip interface and the machined surface. Instead, a similarity in the percentage of the elastically recovered groove surface and the reduction in thrust forces suggests that the phenomenon may be correlated.

Figure 7 illustrates a breakdown of the two-dimensional elliptical vibration-assisted orthogonal cutting process where the tool engages the workpiece with the defined cutting depth at the start of the cycle in Figure 7(a). The elliptical motion of the vibration drives the tool forward to remove material (Figure 7(b)) before the tool retracts away from the workpiece in Figure 7(c). In the final step of the cycle, the tool advances forward once again to the new starting position of the subsequent vibratory cycle (Figure 7(d)). Figure 7(c) also includes the elastically recovered machined surface, which results in the plunging of the tool into the additional layer as it prepares for the subsequent cycle.

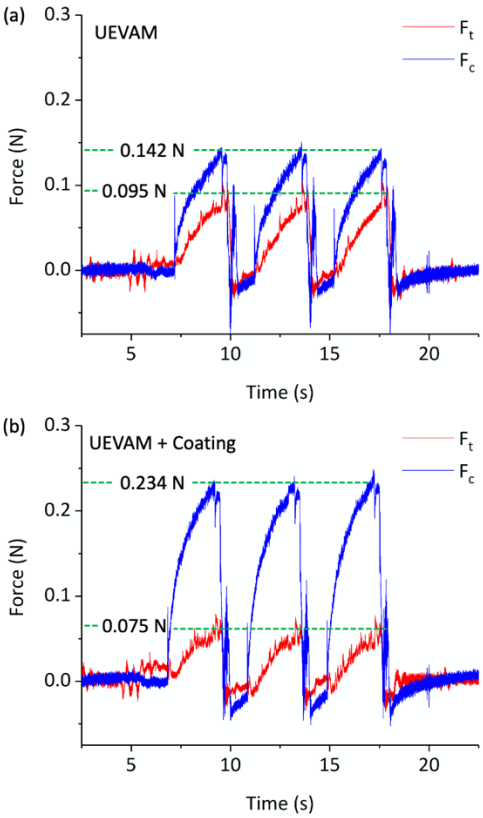

Figure 6. Measured cutting (F_c) and thrust (F_t) forces during: (a) ultrasonic elliptical vibration-assisted machining (UEVAM), and (b) UEVAM of the sample coated with epoxy resin

In this scenario of UEVAM, the plunging of the tool likely induces the additional thrust forces that were recorded in Figure 6. However, the implementation of the coating alongside UEVAM results in lower elastic recovery of the machined surface, and the reduced thrust forces will be induced onto the cutting tool. Cutting forces were also likely to be affected by the elastically recovered surface, which should reveal larger cutting forces in UEVAM as compared to UEVAM with the coating. However, the layer of epoxy coating (4 µm) ahead of the cutting direction, which is significantly thicker than the undeformed chip thickness (0.5 µm), would indefinitely induce a substantial amount of cutting forces as reflected in Figure 6(b).

3.4. Integrated effect

At this juncture, the benefit of the integrated augmentation to micro-cutting in improving machining form accuracy was established and validated through surface measurements and observation in thrust forces. Hence, it is important to understand the potential cause for this positive result.

The elastic recovery, otherwise known as the spring back (Equation 2), was previously modelled as a function of the work material hardness (*H*) and modulus of elasticity (*E*) [5, 6].

$$s = k_1 r \frac{H}{E} \quad (2)$$

where k_1 is a scaling constant and r is the tool-edge radius. For the elastic recovery to decrease, the modulus of elasticity has to substantially increase. The tool-edge radius may be assumed to

be constant as the same cutting tool was used for the orthogonal micro-cutting experiments. Thus, the spring back would depend on the hardness and elastic modulus.

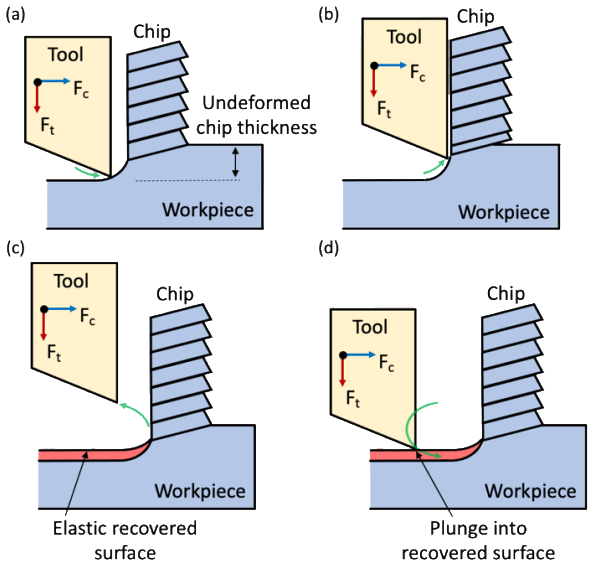

Figure 7. Step-by-step illustration of the orthogonal ultrasonic elliptical vibration-assisted machining cycle with additional considerations for the elastically recovered surface: (a) initial position of a cycle; (b) material removal; (c) tool pull-back; (d) re-entry to initial position

The latter is correlated to interatomic bonding forces, which are strongly affected by temperature. Assuming that the machined surface temperature remains the same under the different cutting conditions, the modulus of elasticity would remain constant and the spring back will be proportional to the material hardness. The larger spring back of the surface machined by UEVAM without the coating indicates that the surface is mechanically harder, which could have been the result of subsurface damage after cutting such as lattice distortion.

Work hardening of the machined surface can be attributed to subsurface damage in the form of lattice distortions or the nucleation of a large density of dislocations [7]. Intuitively, a larger volume of subsurface damaged material would correspond to a harder surface. Interestingly, it was previously reported that the conventionally cut CaF_2 surface with the coating had a 45% reduction in thickness of the subsurface damaged layer [8]. While the reported degree of improvement may differ from the subsurface damage by UEVAM, the relationship between the subsurface damage and hardness may be immediately drawn to explain the reduction in elastic recovery.

Subsurface damage is largely a result of the activation of slip systems under the stress induced during deformation beginning with the primary slip system. While a major portion of the cutting energy is converted into plastic deformation in the primary deformation zone of the cutting process, a subset of the energy also affects the primary slip system in the subsurface region (Figure 8(a)). The coating alters the flow of this stress by inducing additional stresses into the primary deformation zone, which potentially activates secondary slip systems in the region and concentrates a larger proportion of the cutting energy into the primary deformation zone (Figure 8(b)). The remaining energy is then insufficient to affect slip systems in the tertiary deformation zone, and therefore reduces the deformation of the subsurface. This results in lower subsurface damage in the machined surface, which adequately explains the reduction in elastic recovery (Equation 2). The proposed theory will require further validation beyond this work, but the results of the integrated manufacturing technique are proven to be beneficial to improving the form accuracy in ultra-precision machining.

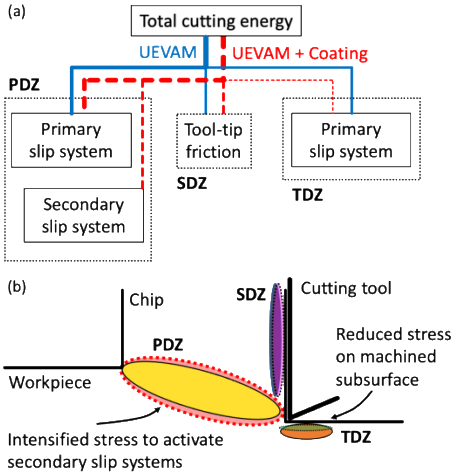

Figure 8. Schematic illustrating the proportion of energy consumed in the different deformation zones during cutting: (a) flow chart for the dissipation of stored elastic strain energy to the primary deformation zone (PDZ), secondary deformation zone (SDZ), and tertiary deformation zone (TDZ); (b) 2D schematic of the deformation zones during cutting

4. Conclusions

The integration of ultrasonic elliptical vibration-assisted machining (UEVAM) and the pre-coating of the workpiece in micro-cutting of single-crystal calcium fluoride was proven to successfully improve the form accuracy. The surface prepared by UEVAM had a larger deviation from the designed geometry by 18.4% as compared to the integration, which boasted a minor deviation of 5%. The impact of the elastically recovered surface was evident from the 21.1% increase in thrust forces by UEVAM. The effect of the coating was proposed to promote the activation of secondary slip systems in the primary deformation zone, which consumes more cutting energy and reduces the energy for deformation of the machined surface and its corresponding elastic recovery. The benefit of the integration is evidently capable of augmenting ultra-precision machining technology.

Acknowledgements

This work was supported by Singapore Ministry of Education AcRF Fund (R-265-000-686-114; MOE-T2EP50120-0010) and Agency for Science, Technology and Research, Singapore (Grant No.: A19E1a0097). The author also appreciates the support from Dr Hao Wang and Mr Yeo Eng Huat Nelson toward this research.

References

[1] Huo D and Cheng K 2019 *Proc. Inst. Mech. Eng. Part C J. Mech. Eng. Sci.* **233** 4079-80

[2] Suzuki N, Nakamura A, Shamoto E, Harada K, Matsuo M and Osada M 2004 *Micro-Nanomechatronics Hum. Sci. 2004 Fourth Symp.* 113-38

[3] Lee Y J, Kumar A S and Wang H 2021 *Int. J. Mach. Tools Manuf.* **168** 103787

[4] Zhang X, Sui H, Zhang D and Jiang X 2018 *Int. J. Adv. Manuf. Technol.* **95** 3929-41

[5] Zhang X, Arif M, Liu K, Kumar A S and Rahman M 2013 *Int. J. Mach. Tools Manuf.* **69** 57-66

[6] Arcona C and Dow T A 1998 *J. Manuf. Sci. Eng.* **120** 700-7

[7] Yan J, Asami T, Harada H and Kuriyagawa T 2009 *Precis. Eng.* **33** 378-86

[8] Lee Y J, Chong J Y, Chaudhari A and Wang H 2020 *Int. J. Precis. Eng. Manuf. Technol.* **7** 1019-29